Cell Reports
Medicine

Report

Serotypic evolution of measles virus is constrained by multiple co-dominant B cell epitopes on its surface glycoproteins

Graphical abstract

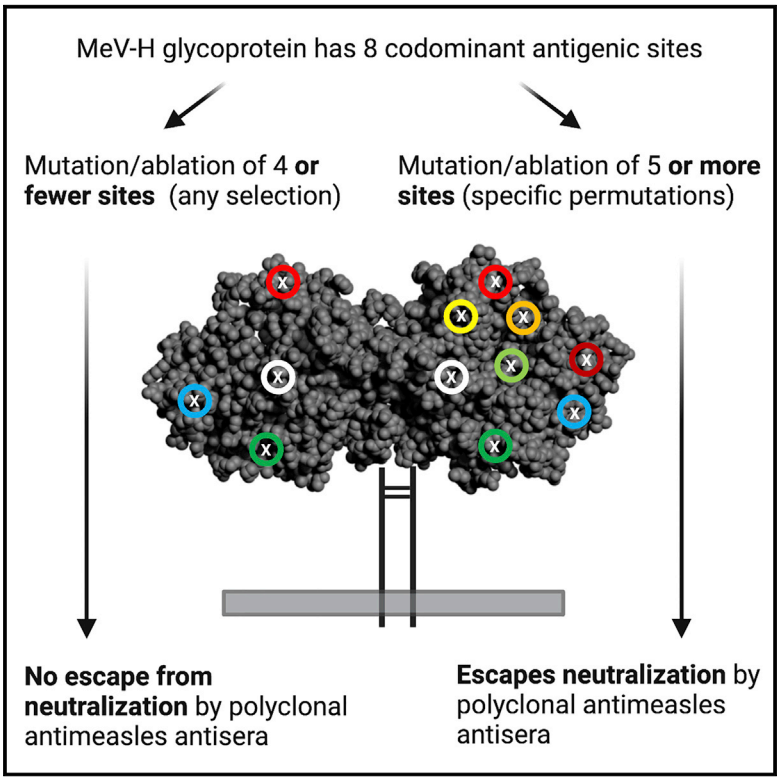

Highlights

- The 8 known MeV-H protein antigenic sites and all permutations of 7 could be ablated
- Neutralization studies show antigenic sites in MeV-H are serologically co-dominant
- Ablation of at least 5 co-dominant sites is required to escape serum neutralization
- Natural evolution of a vaccine-bypassing MeV strain is a highly improbable event

Authors

Miguel Ángel Muñoz-Alía, Rebecca A. Nace, Lianwen Zhang, Stephen J. Russell

Correspondence

alia.miguel@mayo.edu (M.Á.M.-A.), sjr@mayo.edu (S.J.R.)

In brief

Live attenuated measles virus (MeV) vaccines have remained protective for 60 years because wild-type MeVs have remained antigenically monotypic. Muñoz-Alía et al. show that escape from serum neutralization requires elimination of at least five co-dominant antigenic sites in the hemagglutinin (H) glycoprotein. They conclude that emergence of new serotypes is highly unlikely.

Muñoz-Alía et al., 2021, Cell Reports Medicine 2, 100225
April 20, 2021
https://doi.org/10.1016/j.xcrm.2021.100225

CellPress

Cell Reports Medicine

CellPress
OPEN ACCESS

Report

Serotypic evolution of measles virus is constrained by multiple co-dominant B cell epitopes on its surface glycoproteins

Miguel Ángel Muñoz-Alía,[1,*] Rebecca A. Nace,[1] Lianwen Zhang,[1] and Stephen J. Russell[1,2,3,*]
[1]Department of Molecular Medicine, Mayo Clinic, Rochester, MN 55905, USA
[2]Department of Molecular Medicine and Division of Hematology, Mayo Clinic, Rochester, MN 55905, USA
[3]Lead contact
*Correspondence: alia.miguel@mayo.edu (M.Á.M.-A.), sjr@mayo.edu (S.J.R.)
https://doi.org/10.1016/j.xcrm.2021.100225

SUMMARY

After centuries of pestilence and decades of global vaccination, measles virus (MeV) genotypes capable of evading vaccine-induced immunity have not emerged. Here, by systematically building mutations into the hemagglutinin (H) glycoprotein of an attenuated measles virus strain and assaying for serum neutralization, we show that virus evolution is severely constrained by the existence of numerous co-dominant H glycoprotein antigenic sites, some critical for binding to the pathogenicity receptors SLAMF1 and nectin-4. We further demonstrate the existence in serum of protective neutralizing antibodies targeting co-dominant fusion (F) glycoprotein epitopes. Lack of a substantial reduction in serum neutralization of mutant measles viruses that retain even one of the co-dominant antigenic sites makes evolution of pathogenic measles viruses capable of escaping serum neutralization in vaccinated individuals extremely unlikely.

INTRODUCTION

Measles virus (MeV) is a highly transmissible airborne pathogen that spreads systemically and causes transient immune suppression.[1,2] Childhood infection is associated with significant mortality, and MeV elimination remains a high priority for the World Health Organization.[3] MeV cell entry via the immune cell receptor SLAMF1 (CD150) drives measles immunopathogenesis,[4] whereas a second epithelial cell receptor, nectin-4 (PVRL4), is exploited for virus transmission.[5] Receptor attachment and virus entry are mediated by the concerted action of the hemagglutinin (H) and fusion (F) surface glycoproteins.[2] The MeV polymerase has a high mutation rate and a correspondingly high frequency of monoclonal neutralizing antibody (nAb) escape mutants but has nevertheless remained monotypic.[6,7] Vaccination with a lab-adapted isolate of the genotype A strain MeV, isolated from the throat of David Edmonston in 1954, still confers full protection against all currently circulating genotypes. The evolutionary stability of MeV remains poorly understood but could be due to the inability of its surface glycoproteins to tolerate sequence modification,[8–11] the multiplicity of B cell epitopes displayed on its surface, and/or the low likelihood of mutational escape from combined B and T cell-mediated antiviral defenses.

Here, to elucidate the serotypic constraints on MeV evolution, we introduced mutated H glycoproteins into a vaccine-lineage MeV strain using reverse genetics. The Edmonston vaccine lineage was originally attenuated by serial passage on SLAMF1-negative, nectin-4-negative cell substrates and adapted to also use CD46 as a receptor. MeV-Moraten was selected for the current study because it is currently the dominant vaccine strain used in the western hemisphere and has an outstanding biosafety profile when administered to measles-naive individuals. Particularly important for the envelope engineering studies described in this report, the vaccine attenuated phenotype is highly stable, and there are no recorded cases of a MeV vaccine strain reverting to a pathogenic phenotype or person-to-person vaccine transmission.[12] Mechanistically, vaccine attenuation is multifactorial, arising from acquisition of CD46 tropism,[13] inactivating mutations in V and C immune combat proteins, mutations in the L (polymerase) protein,[14] and mutations in noncoding sequences.[15]

RESULTS

To facilitate detailed analysis of MeV-H neutralization, we assembled a comprehensive set of 30 published anti-MeV-H monoclonal antibodies known to neutralize virus infectivity. For antibodies with unknown target epitopes, we propagated the virus in the presence of the antibody, selected escape mutants, and sequenced them for epitope identification. Subsequently, we introduced increasing numbers and varying combinations of epitope escape mutations into an antigenically advanced and relatively malleable MeV-H protein obtained from the H1 genotype of MeV (Figure 1A; Table S1),[16] which, to facilitate evaluation of mutants with disrupted SLAMF1 and nectin-4 receptor binding sites, had been engineered to bind to CD46 by introducing the mutations N481Y, H495R, and S546G (Figure S1).

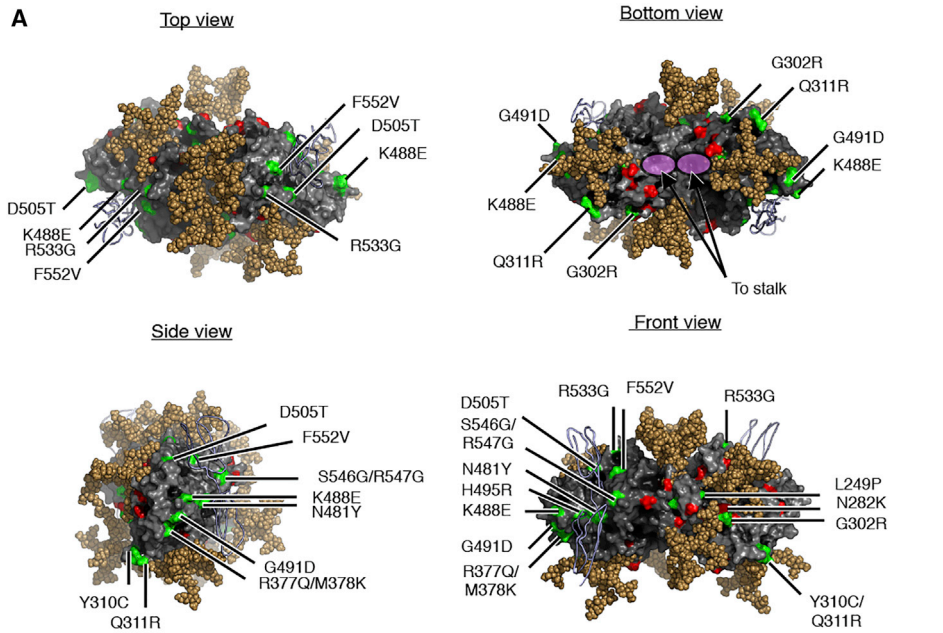

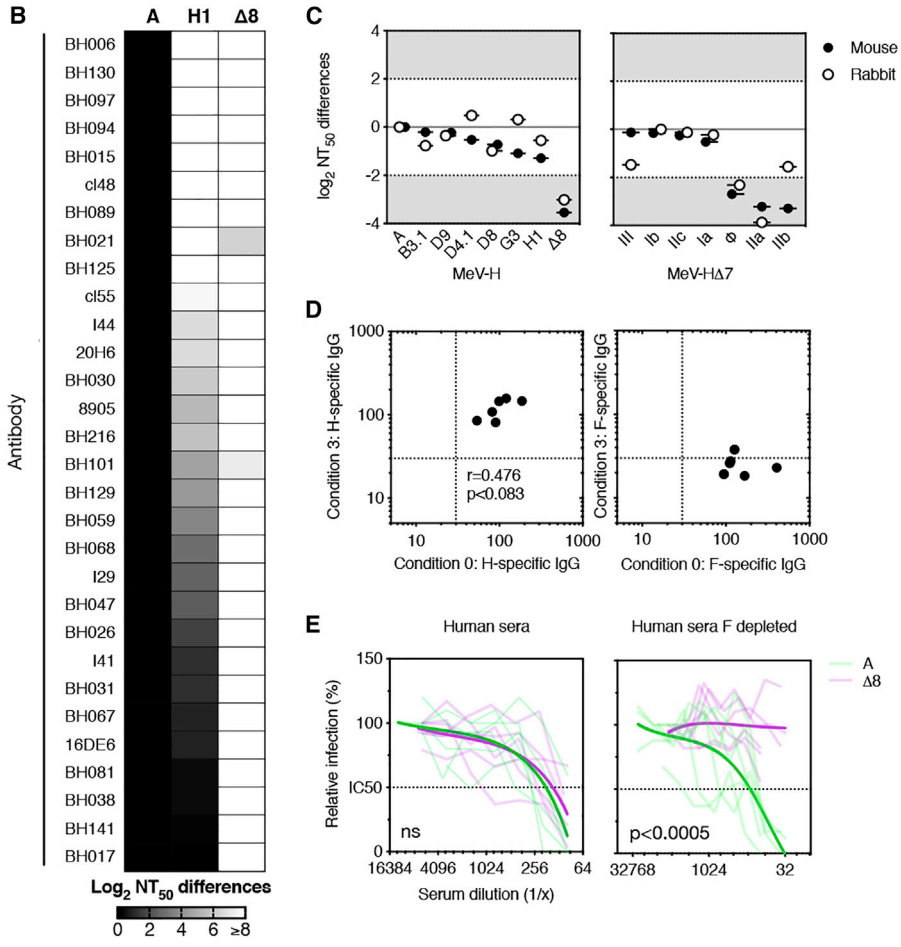

(legend on next page)

We thereby generated a CD46-tropic MeV (MeV-H Δ8) in which all 7 previously reported antigenic sites[16] plus an eighth site (IIc) identified in the course of the current study were disrupted successfully (Figures 1 and S2). Neutralization assays confirmed that viruses encoding MeV-H Δ8 showed decreased susceptibility to neutralization by all 30 mAbs (Figure 1B).

Interim analysis of the neutralization of mutated viruses by anti-MeV-H antisera has revealed that disruption of 4 or fewer antigenic sites does not abrogate polyclonal antibody neutralization.[16–18] However, in MeV-H Δ8, we observed an 8-fold reduction in the neutralization titer of mouse anti-MeV-H antiserum (Figure 1C). We therefore back-mutated the disrupted antigenic sites to create a panel of Δ7 viruses, each one uniquely presenting a single intact antigenic site. Interestingly, with the exception of the Δ7 viruses retaining antigenic sites Φ, IIa, or IIb, all of the other four Δ7 viruses were serologically indistinguishable from the parental virus (Figure 1C). These results were replicated using sera from MeV-H-immunized rabbits (Figure 1C). Thus, simultaneous disruption of at least five antigenic sites is required to manifest resistance to neutralization by MeV-H antisera.

We next sought to determine whether polyclonal sera from measles vaccinees paralleled the reactivity of mouse and rabbit antisera. Serum samples from Dutch individuals (n = 6, cohort 1) were tested before and after depletion of MeV-F-reactive antibodies (Figure 1D). Although MeV-F–depleted human serum retained its neutralization potency against viruses displaying MeV-H genotype A, the Δ8 viruses were neutralized less readily (7-fold reduced susceptibility after averaging individual titers) (Figure 1E).

Because antigenic site III is known to overlap with the SLAMF1 and nectin-4 receptor-interacting surfaces of MeV-H,[19] elimination of B cell epitopes in this region was expected to negatively affect binding to these critical pathogenicity-determining receptors. We therefore examined the receptor tropisms of the Δ8 variant and of the Δ7 variants exhibiting reduced susceptibility to serum neutralization (Figure S3). None of these viruses were able to mediate infection via SLAMF1, indicating that the emergence of a pathogenic MeV strain with reduced susceptibility to serum neutralization would require the virus to reconfigure the receptor-interacting residues in antigenic site III in a way that destroys the dominant B cell epitopes it shares with existing MeV vaccine strains while retaining nectin-4 and SLAMF1 receptor binding affinities.

Having demonstrated that the multiply mutated MeV-H Δ8 protein could not interact with pathogenicity-determining MeV receptors, we next sought to eliminate the confounding effect of nAbs recognizing the MeV-F glycoprotein (e.g., anti-MeV-F nAb mask antigenic drift of MeV-H) (Figure 2). To achieve this, we substituted the MeV-F gene with the corresponding gene from canine distemper virus (CDV). Mutations were introduced into the CDV-F and MeV-H coding sequences to restore and optimize the fusogenicity of this heterologous F/H pairing. This virus, hereafter called MR (Moraten resurfaced), was subjected to Sanger sequencing and protein composition analysis to confirm its identity. Propagation of the MeV MR virus on Vero cells was slowed significantly versus a comparable virus incorporating an unmodified MeV-H genotype A protein (Figure 3A). Propagation of MeV-H Δ8 with the parental MeV-F glycoprotein was impaired similarly, indicating that mutation of multiple surface residues in MeV-H compromised protein folding and/or function (Figure 3A).

We next tested whether MeV-MR was resistant to human serum from vaccinated Dutch (n = 13, cohort 1), Minnesotan (n = 6, cohort 2), and Hispanic individuals (n = 4, cohort 3) using an improved luciferase-based infection neutralization assay (Figure 3B). Neutralization titer values of the tested serum samples gave an overall geometric mean titer 5.5-fold lower against MeV-MR versus MeV-A (Figure 3C), suggesting that resistance to neutralization of MeV-MR is fully manifested only at or below a MeV-A neutralization titer of 679 mIU/mL (Figure 3C).

Interestingly, measles-immune serum does retain some level of neutralizing activity against MeV-MR, suggesting that it may also contain protective antibodies directed against subdominant epitopes in the MeV-H glycoprotein. To test this, we inoculated MeV-MR or MeV-A viruses into immunocompetent Ifnar^{tm}-CD46Ge mice, harvested sera 4 weeks later, and tested for the presence of immunoglobulin G (IgG) antibodies directed against the nucleocapsid (MeV-N) or MeV-H proteins of pathogenic MeVs (Figure S4). Interestingly, the data confirm that antisera raised against MeV-MR do weakly crossreact with wild-type MeV-H, indicating that subdominant B cell epitopes may play a significant role in MeV defense. Conversely, antibodies raised

Figure 1. Rational design of MeV-H Δ8

(A) Model of the dimeric structure of the MeV-H Δ8. N-linked sugars are depicted as brown spheres (N168, N200, N215, and N416). Amino acid differences with regard to the MeV-H vaccine Moraten strain are indicated; red areas are MeV-H-genotype-H1-specific changes, and green areas are engineered nAb escape mutations.

(B) Neutralization sensitivity of viruses encoding MeV-H A, H1, and Δ8 against a panel of 30 mAbs. Boxes are shaded according to differences in $\log_2$ of the antibody concentration required to inhibit viral infection by 50% (neutralizing antibody titer at 50% inhibition [NT_{50}]).

(C) Neutralization sensitivity of viruses encoding genotype-specific MeV-H (A, B3.1, D4.1, D8, G3, and H1; left panel) in comparison with those expressing MeV-H Δ8 or (right panel) MeV-H Δ7 mutants (indicated is the antigenic site still remaining intact) against mouse (black dots) and rabbit (empty dots) sera raised against MeV-H genotype A. A difference of 2 $\log_2$ or more (gray-shaded region) is considered antigenically significant.

(D) MeV glycoprotein-specific antibodies. Shown are IgG antibody levels after incubating MeV-immune human sera from the Dutch cohort with cells expressing MeV-F (condition 3) and comparing their levels with those of untreated human sera (condition 0). Values of less than 30 were considered negative for antibody binding (lower crosshairs).

(E) Neutralization sensitivity of MeV A or Δ8 against MeV-immune human sera after depletion no depletion of MeV-F-specific antibodies. Serum samples were the same as those shown in (D). Each semitransparent line indicates a different individual (n = 6), and the solid trend lines represent the nonlinear regression fitting against MeV A (green) or Δ8 (magenta).

Statistical significance ($p < 0.0005$) was determined by Wilcoxon matched-pair signed rank test.

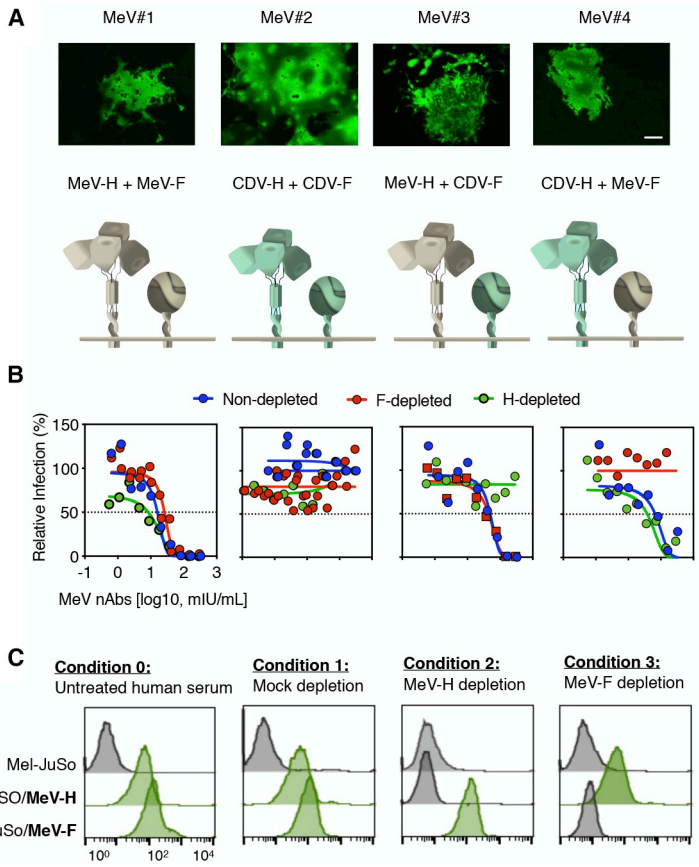

Figure 2. Role of MeV-H and MeV-F in virus neutralization

(A) Representative syncytia and schematic representation of isogenic recombinant MeV encoding MeV envelope glycoproteins (MeV#1), CDV (MeV#2), or chimeric viruses (MeV#3 and MeV#4). Scale bar, 100 μm.

(B) Virus neutralization assay of envelope exchange viruses. MeV#1–MeV#4 were used to test neutralization sensitivity against pooled human AB sera depleted of antibodies against MeV-H or MeV-F.

(C) MeV glycoprotein specificity of pooled human AB sera. Conditions and IgG-specific levels are described and were determined as in Figure 1. The remaining MeV coat-specific antibodies were tested again to confirm successful depletion. Data are shown as histogram plots.

against MeV-A were able to crossreact with subdominant epitopes in the MeV-H Δ8 protein.

Because MeV-MR is partially resistant to neutralization by measles-immune human sera, it was important to confirm that, like MeV-Δ8, it lacks the ability to use the pathogenicity-determining receptors SLAMF1 and nectin-4 and enters cells exclusively via CD46. This was confirmed using Chinese hamster ovary (CHO) cells expressing CD46, nectin-4, or SLAMF1, where, unlike MeV-A, MeV-MR infected only cells expressing CD46 (Figure 3D). This selective tropism is particularly interesting because previous reports have claimed that nectin-4 tropism could not be eliminated independent of CD46 tropism.[20,21] We therefore measured the densities of CD46 and nectin-4 receptors on our respective CHO cell transfectants and found them to be equivalent (Figure S1B). Co-transfecting plasmids encoding MeV-F and MeV-H Δ8 confirmed that intercellular fusion occurred only in CD46-positive and not nectin-4-positive CHO cells (Figure 3E) and was similar to CD46 of nonhuman primate origin.

Further mechanistic studies into the discrimination of CD46 over nectin-4 showed that MeV-H Δ8 bound more strongly to CD46 than to nectin-4 and negligibly to SLAMF1. This contrasted with the binding pattern for MeV-H A (Figure 3F) and suggested that MeV-H Δ8 discriminates between CD46 and nectin-4 via differences in its binding affinities to each of these receptors. We identified no second-site mutations in known contact residues to explain this unexpected segregation of CD46 and nectin-4 tropisms and therefore postulate that the phenotype may be partially attributable to specific noncontact residues in the MeV-H protein of genotype H1.

Measles-immune human serum is known to negate seroconversion in infants during the first year of life and negates the therapeutic effect of systemically administered oncolytic MeV. In the latter case, the complete response of an individual with multiple myeloma following a single intravenous infusion of MeV at the Mayo Clinic was associated with lack of detectable neutralizing anti-measles antibodies at baseline and a high baseline frequency of measles-reactive T cells.[22] Hence, we sought to investigate the effect of passive immunization on the infectivity of the MR virus versus the MeV vaccine. Although passive immunization with MeV antisera led to a decrease in luciferase signal from MeV-A, there was no reduction in the case of the MeV-MR (Figure 4). Accordingly, systemically administered MeV-MR in tumor-bearing mice could reach its target (the tumor cells) in the presence of passive antibodies.

DISCUSSION

By engineering the surface glycoproteins of a MeV vaccine, we elucidated a number of critical factors determining the remarkable antigenic stability of this monotypic virus. First, MeV has numerous immunologically codominant antigenic sites on its H and F surface glycoproteins. Second, antibodies to each of the seven known antigenic regions on the H glycoprotein are capable of neutralizing virus infectivity. Third, MeVs retaining even a single immunodominant antigenic site on the H glycoprotein remain fully susceptible to neutralization by measles immune human serum. Fourth, the receptor binding surface of the MeV-H glycoprotein is itself an immunodominant antigenic site. Hence, MeVs cannot escape their susceptibility to neutralization by measles-immune human serum unless they also lose their tropism for the pathogenicity-determining receptors SLAMF1 and nectin-4.

Given that a minimum of five immunodominant antigenic sites must be disrupted to affect the susceptibility of MeV-H to serum neutralization, the probability of it happening naturally is

CellPress
OPEN ACCESS

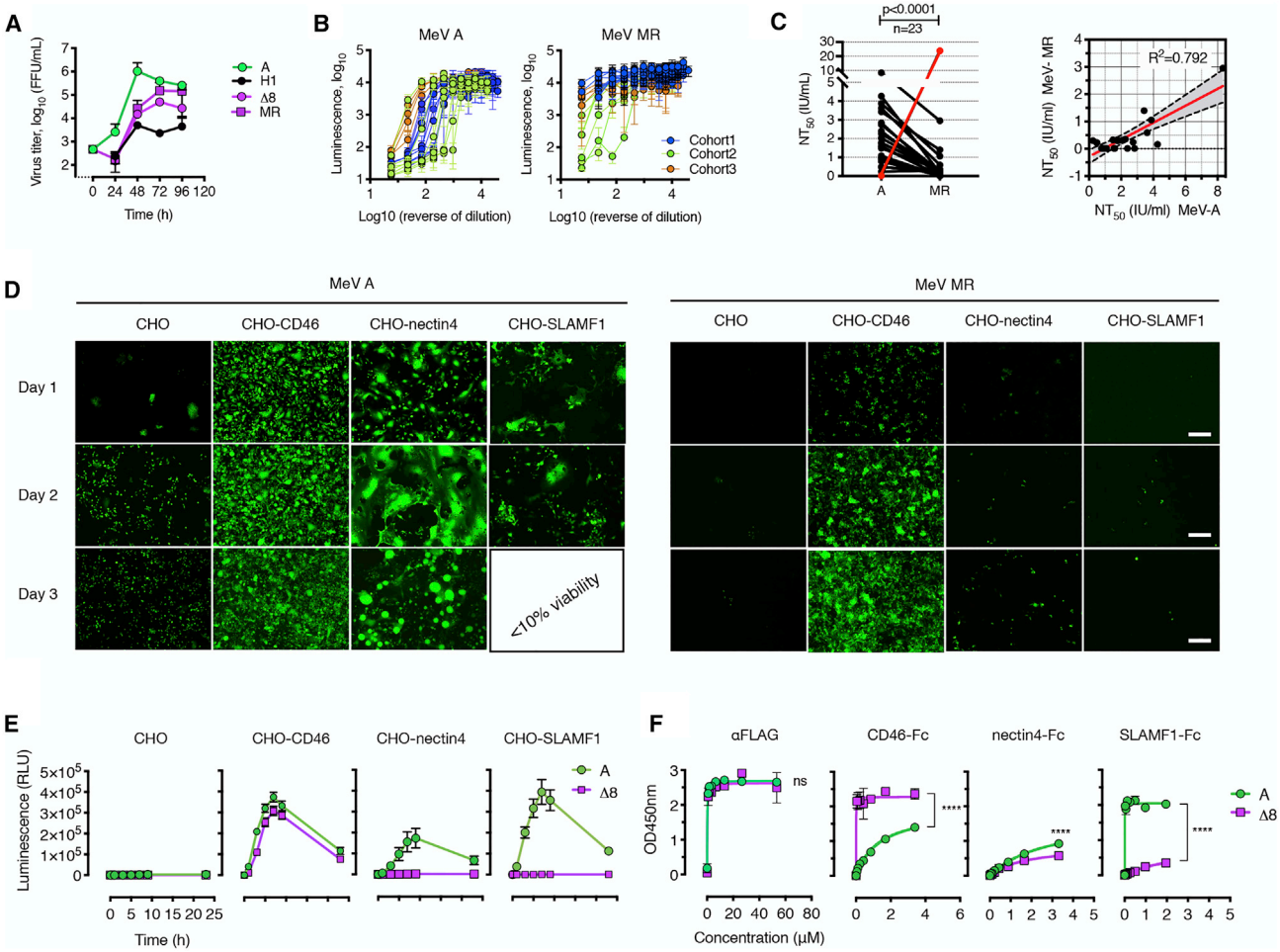

Figure 3. *In vitro* characterization of the MR virus

(A) Replication kinetics of viruses on Vero/hSLAMF1 infected at an MOI of 0.03. MeV A, H1, and Δ8 denote MeVs expressing the corresponding MeV-H genes and MeV-F genotype A, whereas the MR virus encodes MeV-H Δ8 plus CDV-F. Values and error bars represent the mean and standard deviation (SD), respectively.

(B) Neutralization activity of human serum samples. Samples belonging to different cohorts are colored-coded. Mean ± SD

(C) Left panel: NT_{50} values of MeV-immune human sera against the MeV A and MR. Each line represents an individual sample (n = 23). The red line shows ferret serum anti-CDV, used as a control for neutralization. Statistical significance was inferred by a two-tailed paired t test. Right panel: correlation between NT_{50} for the vaccine virus and the MR virus. $p < 0.001$ for Pearson and Spearman correlation tests. The red curved line is the linear regression line, and dotted lines indicate the 95% confidence interval (CI) for the regression analysis.

(D) CHO cells expressing different MeV receptors were infected at an MOI of 1. Images were obtained 3 days after infection. Scale bar, 200 μm.

(E) Kinetics fusion assay after co-expression of MeV-F with MeV-H A or Δ8. Mean ± SD.

(F) Binding of MeV receptor-Fc to MeV-H protein, monitored by optical density (OD). The FLAG epitope in MeV-H was used as a coating control. Data are presented as mean ± SD and were fitted to a 1-site mode of total binding ($R^2 > 0.99$). Statistical significance was determined using the Holm-Sidak multiple comparison test. ns, not significant; ****$p < 0.001$.

vanishingly small. Further, simultaneous disruption of fewer than five major antigenic sites would confer no selective advantage on the virus, making stepwise evolution an unrealistic pathway to achieve a neutralization-resistant phenotype. However, even a MeV insensitive to anti-MeV-H antibodies would still be efficiently neutralized by MeV-F-specific antibodies in immune human sera and, even more critical, would lack the SLAMF1 and nectin-4 receptor tropisms required for pathogenicity and transmission. In addition, the requirement of H-F cooperation in fusion triggering is likely an additional constraint to antigenic evolution. This presents a stark contrast with results from other respiratory RNA viruses, such as influenza and coronavirus, where a much smaller number of amino acid substitutions at key positions within a single virus-embedded glycoprotein can cause escape from polyclonal antibody responses in sera.[23–30] We therefore conclude that there is a near-zero probability for the accidental emergence of a pathogenic MeV capable of evading vaccine-induced immunity.

Limitations of study

Our study focuses entirely on antibodies capable of neutralizing virus infectivity *in vitro*, largely ignoring non-nAbs, which are a

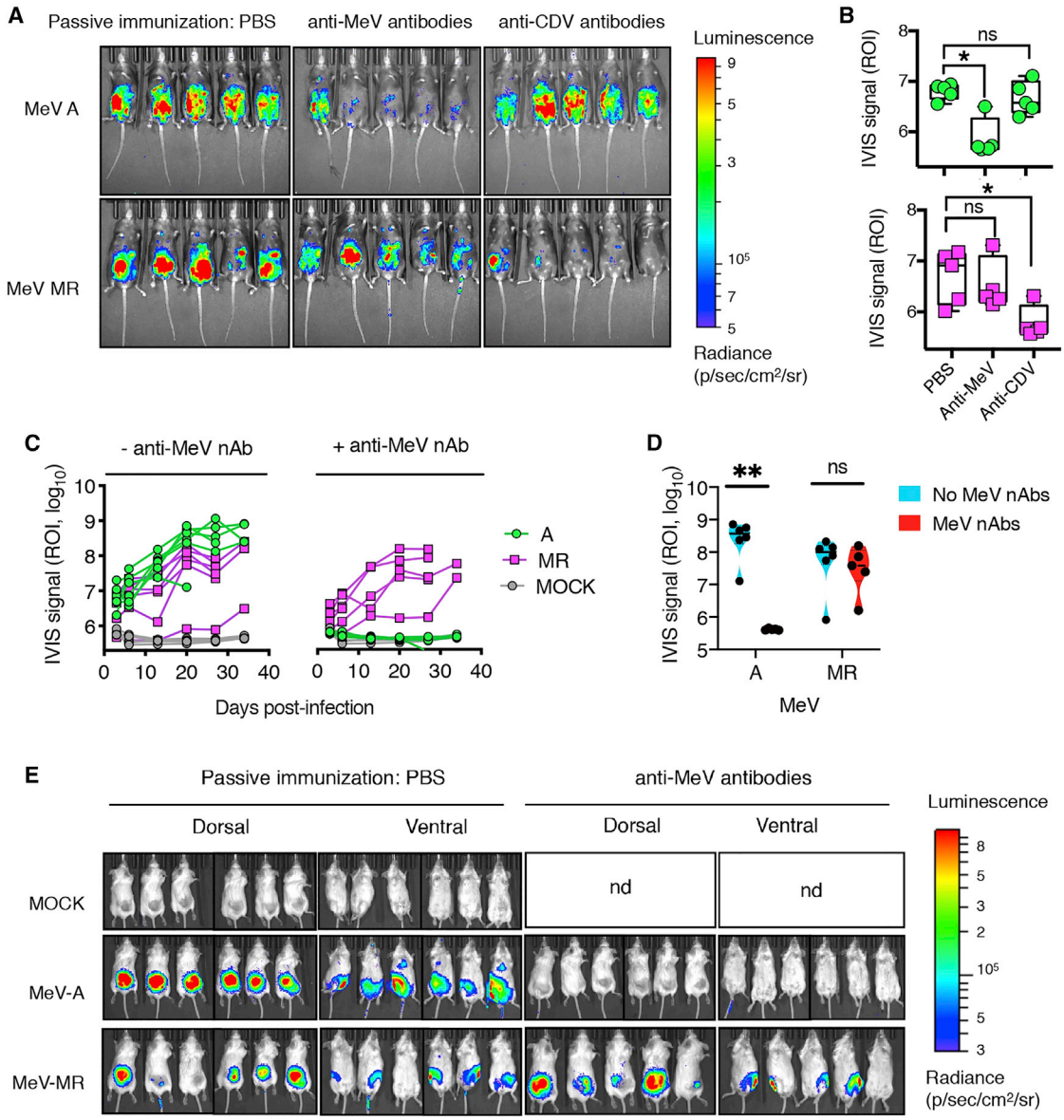

Figure 4. The MR virus shows resistance *in vivo* to neutralization by MeV A-induced antibodies

(A) Bioluminescence signal of a virally encoded firefly luciferase (Fluc) signal in Ifnar^{tm}-CD46Ge mice pre-treated or not (PBS group) with guinea pig anti-MeV or ferret anti-CDV nAb-containing serum. The images were recorded 3 days after infection and show absence of a bioluminescence signal for MeV A in the presence of MeV antibodies, whereas the presence of CDV antibodies, but not MeV antibodies, inhibited the virus MR.

(B) Quantification of the bioluminescence signal emitted from the abdominal and ventral area or region of interest (ROI) from each mouse infected with MeV in the presence or absence of passive immunity. PBS represents mock-immunized mice. *$p < 0.005$, as calculated with Dunnett's corrected 1-way ANOVA with 12 degrees of freedom.

(C) Bioluminescence quantitative signal (photons) of severe combined immunodeficiency (SCID) mice bearing subcutaneous KAS 6/1 cells treated intravenously with one dose of the indicated rMeV(Fluc) or PBS. Mice in the relevant group also received anti-MeV antibodies (MeV-specific guinea pig antiserum) intraperitoneally 3 h before MeV injection.

(D) Comparative analysis of the bioluminescence signal was determined on day 20 for MeV A and MeV MR in the absence or presence of anti-MeV antibodies. Nd, not done. **$p = 0.0064$, as determined by two-way ANOVA with Sidak's multiple comparisons test.

(E) Representative bioluminescence images of tumor-bearing SCID mice treated with MeV.

major component of the humoral immune response, and completely disregarding cellular immunity. Although several studies have shown that nAbs are the best correlate of protection against measles,[31,32] there may be significant *in vivo* contributions from antibody-dependent cellular cytotoxicity (ADCC), complement-dependent cytolysis, and phagocytosis of opsonized virions. Another limitation of our study is that we focused primarily on co-dominant B cell epitopes on the MeV-H

glycoprotein that facilitate direct neutralization by antibodies, and we did not attempt to characterize or determine the number of comparable co-dominant B cell epitopes on the MeV-F glycoprotein. Although we did not study cellular immunity, T cells are not thought to contribute significantly to measles prevention, as exemplified by a study in non-human primates, where T cell immunity did not protect from acute disease but facilitated recovery from infection.[33] A final limitation of our study is that, although we elucidated the low probability that a new MeV serotype could evolve naturally by mutation and selection, we cannot exclude the possibility that MeV could undergo a recombination event with a related paramyxovirus to acquire new F and H glycoproteins that are serologically non cross-reactive with the MeV F and H glycoproteins, escaping antibody neutralization by a different mechanism.

STAR★METHODS

Detailed methods are provided in the online version of this paper and include the following:

- KEY RESOURCES TABLE
- RESOURCE AVAILABILITY
  - Lead contact
  - Materials availability
  - Data and code availability
- EXPERIMENTAL MODEL AND SUBJECT DETAILS
  - Biosafety Statement
  - Human samples
  - Cells and viruses
  - Organism
- METHOD DETAILS
  - Constructs and rescue of recombinant MeVs
  - Fusion assay
  - Fluorescence-activated cell sorting analysis and quantification of cell surface molecules
  - Recombinant proteins and binding assays
  - Assessment of F interaction with H proteins
  - Passive Immunization and *In Vivo* Imaging
  - Serologic Assays
  - Structural Modeling
- QUANTIFICATION AND STATISTICAL ANALYSIS

SUPPLEMENTAL INFORMATION

Supplemental information can be found online at https://doi.org/10.1016/j.xcrm.2021.100225.

ACKNOWLEDGMENTS

We sincerely thank Mark J. Federspiel, PhD, for mAb cl48; Patricia Devaux, PhD, for cl55; Ianko D. Iankov, MD, PhD, for mAb 20H6; Prof. Claude Muller, MD, for the remaining murine nAbs as well as discussions; Veronica von Messling, PhD, for the rabbit anti-F antibody for western blotting; Roberto Cattaneo, PhD, for Vero/dogSLAMtag, measles virus antigenome plasmids, and rabbit anti-MeV antibodies for Western blotting; Rik L. de Swart, PhD, for the Mel-JuSo cell lines, human serum samples, and antibodies C28-10-8 and F3-5; the Mayo Clinic Biobank for serum samples from the Minnesotan cohort; M. Cristine Charlesworth, PhD, and Benjamin J. Madden (Mayo Clinic Proteomics Core) for purification and mass spectrometry of soluble receptors-Fc; Zene Matzuda, MD, PhD, DSc, for the split luciferase plasmids; and Eugene Bah for assistance with the initial quantitative fusion assays and useful discussions. We also thank the Mayo Clinic Biosafety Committee and anonymous reviewers for critical reading of the manuscript and helpful discussions. This work was funded by grants from Al and Mary Agnes McQuinn and the Mayo Clinic. The funders had no role in study design, data collection and interpretation, or the decision to submit the work for publication.

AUTHOR CONTRIBUTIONS

Conceptualization, M.Á.M.-A. and S.J.R.; methodology, M.Á.M.-A. and S.J.R.; validation, M.Á.M.-A. and S.J.R.; investigation: M.Á.M.-A., R.A.N., and L.Z.; analysis, M.Á.M.-A. and S.J.R.; resources, M.Á.M.-A. and S.J.R.; writing, review, and editing, M.Á.M.-A. and S.J.R.; funding acquisition, S.J.R.; approval of the final manuscript, all authors.

DECLARATION OF INTERESTS

M.Á.M.-A. and S.J.R. are inventors in a patent application filed by the Mayo Clinic relating to the virus described in this report (WO2018212842A1) that has been out-licensed. S.J.R. is a founder and equity holder of Vyriad.

INCLUSION AND DIVERSITY

We worked to ensure sex balance in the selection of non-human subjects. One or more of the authors of this paper self-identifies as an underrepresented ethnic minority in science.

Received: November 16, 2020
Revised: January 11, 2021
Accepted: March 4, 2021
Published: March 30, 2021

REFERENCES

1. Mina, M.J., Kula, T., Leng, Y., Li, M., de Vries, R.D., Knip, M., Siljander, H., Rewers, M., Choy, D.F., Wilson, M.S., et al. (2019). Measles virus infection diminishes preexisting antibodies that offer protection from other pathogens. Science *366*, 599–606.
2. Rota, P.A., Moss, W.J., Takeda, M., de Swart, R.L., Thompson, K.M., and Goodson, J.L. (2016). Measles. Nat. Rev. Dis. Primers *2*, 16049.
3. Patel, M.K., Dumolard, L., Nedelec, Y., Sodha, S.V., Steulet, C., Gacic-Dobo, M., Kretsinger, K., McFarland, J., Rota, P.A., and Goodson, J.L. (2019). Progress Toward Regional Measles Elimination - Worldwide, 2000-2018. MMWR Morb. Mortal. Wkly. Rep. *68*, 1105–1111.
4. Leonard, V.H., Hodge, G., Reyes-Del Valle, J., McChesney, M.B., and Cattaneo, R. (2010). Measles virus selectively blind to signaling lymphocytic activation molecule (SLAM; CD150) is attenuated and induces strong adaptive immune responses in rhesus monkeys. J. Virol. *84*, 3413–3420.
5. Leonard, V.H., Sinn, P.L., Hodge, G., Miest, T., Devaux, P., Oezguen, N., Braun, W., McCray, P.B., Jr., McChesney, M.B., and Cattaneo, R. (2008). Measles virus blind to its epithelial cell receptor remains virulent in rhesus monkeys but cannot cross the airway epithelium and is not shed. J. Clin. Invest. *118*, 2448–2458.
6. Birrer, M.J., Udem, S., Nathenson, S., and Bloom, B.R. (1981). Antigenic variants of measles virus. Nature *293*, 67–69.
7. Schrag, S.J., Rota, P.A., and Bellini, W.J. (1999). Spontaneous mutation rate of measles virus: direct estimation based on mutations conferring monoclonal antibody resistance. J. Virol. *73*, 51–54.
8. Fulton, B.O., Sachs, D., Beaty, S.M., Won, S.T., Lee, B., Palese, P., and Heaton, N.S. (2015). Mutational Analysis of Measles Virus Suggests Constraints on Antigenic Variation of the Glycoproteins. Cell Rep. *11*, 1331–1338.

9. Tahara, M., Burckert, J.P., Kanou, K., Maenaka, K., Muller, C.P., and Takeda, M. (2016). Measles Virus Hemagglutinin Protein Epitopes: The Basis of Antigenic Stability. Viruses *8*, 216.

10. Hashiguchi, T., Kajikawa, M., Maita, N., Takeda, M., Kuroki, K., Sasaki, K., Kohda, D., Yanagi, Y., and Maenaka, K. (2007). Crystal structure of measles virus hemagglutinin provides insight into effective vaccines. Proc. Natl. Acad. Sci. USA *104*, 19535–19540.

11. Tahara, M., Ohno, S., Sakai, K., Ito, Y., Fukuhara, H., Komase, K., Brindley, M.A., Rota, P.A., Plemper, R.K., Maenaka, K., and Takeda, M. (2013). The receptor-binding site of the measles virus hemagglutinin protein itself constitutes a conserved neutralizing epitope. J. Virol. *87*, 3583–3586.

12. Greenwood, K.P., Hafiz, R., Ware, R.S., and Lambert, S.B. (2016). A systematic review of human-to-human transmission of measles vaccine virus. Vaccine *34*, 2531–2536.

13. Schnorr, J.J., Dunster, L.M., Nanan, R., Schneider-Schaulies, J., Schneider-Schaulies, S., and ter Meulen, V. (1995). Measles virus-induced down-regulation of CD46 is associated with enhanced sensitivity to complement-mediated lysis of infected cells. Eur. J. Immunol. *25*, 976–984.

14. Takeda, M., Ohno, S., Tahara, M., Takeuchi, H., Shirogane, Y., Ohmura, H., Nakamura, T., and Yanagi, Y. (2008). Measles viruses possessing the polymerase protein genes of the Edmonston vaccine strain exhibit attenuated gene expression and growth in cultured cells and SLAM knock-in mice. J. Virol. *82*, 11979–11984.

15. Bankamp, B., Takeda, M., Zhang, Y., Xu, W., and Rota, P.A. (2011). Genetic characterization of measles vaccine strains. J. Infect. Dis. *204* (*Suppl 1*), S533–S548.

16. Muñoz-Alía, M.A., Muller, C.P., and Russell, S.J. (2018). Hemagglutinin-specific neutralization of subacute sclerosing panencephalitis viruses. PLoS ONE *13*, e0192245.

17. Lech, P.J., Tobin, G.J., Bushnell, R., Gutschenritter, E., Pham, L.D., Nace, R., Verhoeyen, E., Cosset, F.L., Muller, C.P., Russell, S.J., and Nara, P.L. (2013). Epitope dampening monotypic measles virus hemagglutinin glycoprotein results in resistance to cocktail of monoclonal antibodies. PLoS ONE *8*, e52306.

18. Muñoz-Alía, M.A., Muller, C.P., and Russell, S.J. (2017). Antigenic Drift Defines a New D4 Subgenotype of Measles Virus. J. Virol. *91*, e00209, 17.

19. Muñoz-Alía, M.A., Casasnovas, J.M., Celma, M.L., Carabaña, J., Liton, P.B., and Fernandez-Muñoz, R. (2017). Measles Virus Hemagglutinin epitopes immunogenic in natural infection and vaccination are targeted by broad or genotype-specific neutralizing monoclonal antibodies. Virus Res. *236*, 30–43.

20. Liu, Y.P., Russell, S.P., Ayala-Breton, C., Russell, S.J., and Peng, K.W. (2014). Ablation of nectin4 binding compromises CD46 usage by a hybrid vesicular stomatitis virus/measles virus. J. Virol. *88*, 2195–2204.

21. Mateo, M., Navaratnarajah, C.K., Syed, S., and Cattaneo, R. (2013). The measles virus hemagglutinin β-propeller head β4-β5 hydrophobic groove governs functional interactions with nectin-4 and CD46 but not those with the signaling lymphocytic activation molecule. J. Virol. *87*, 9208–9216.

22. Russell, S.J., Federspiel, M.J., Peng, K.W., Tong, C., Dingli, D., Morice, W.G., Lowe, V., O'Connor, M.K., Kyle, R.A., Leung, N., et al. (2014). Remission of disseminated cancer after systemic oncolytic virotherapy. Mayo Clin. Proc. *89*, 926–933.

23. Huang, K.Y., Rijal, P., Schimanski, L., Powell, T.J., Lin, T.Y., McCauley, J.W., Daniels, R.S., and Townsend, A.R. (2015). Focused antibody response to influenza linked to antigenic drift. J. Clin. Invest. *125*, 2631–2645.

24. Koel, B.F., Burke, D.F., Bestebroer, T.M., van der Vliet, S., Zondag, G.C., Vervaet, G., Skepner, E., Lewis, N.S., Spronken, M.I., Russell, C.A., et al. (2013). Substitutions near the receptor binding site determine major antigenic change during influenza virus evolution. Science *342*, 976–979.

25. Koel, B.F., Mögling, R., Chutinimitkul, S., Fraaij, P.L., Burke, D.F., van der Vliet, S., de Wit, E., Bestebroer, T.M., Rimmelzwaan, G.F., Osterhaus, A.D., et al. (2015). Identification of amino acid substitutions supporting antigenic change of influenza A(H1N1)pdm09 viruses. J. Virol. *89*, 3763–3775.

26. Lee, J.M., Eguia, R., Zost, S.J., Choudhary, S., Wilson, P.C., Bedford, T., Stevens-Ayers, T., Boeckh, M., Hurt, A.C., Lakdawala, S.S., et al. (2019). Mapping person-to-person variation in viral mutations that escape polyclonal serum targeting influenza hemagglutinin. eLife *8*, e49324.

27. Davis, A.K.F., McCormick, K., Gumina, M.E., Petrie, J.G., Martin, E.T., Xue, K.S., Bloom, J.D., Monto, A.S., Bushman, F.D., and Hensley, S.E. (2018). Sera from Individuals with Narrowly Focused Influenza Virus Antibodies Rapidly Select Viral Escape Mutations *In Ovo*. J. Virol. *92*, e00859, 18.

28. Eguia, R., Crawford, K.H.D., Stevens-Ayers, T., Kelnhofer-Millevolte, L., Greninger, A.L., Englund, J.A., Boeckh, M.J., and Bloom, J.D. (2020). A human coronavirus evolves antigenically to escape antibody immunity. bioRxiv. https://doi.org/10.1101/2020.12.17.423313.

29. Andreano, E., Piccini, G., Licastro, D., Casalino, L., Johnson, N.V., Paciello, I., Monego, S.D., Pantano, E., Manganaro, N., Manenti, A., et al. (2020). SARS-CoV-2 escape in vitro from a highly neutralizing COVID-19 convalescent plasma. bioRxiv. https://doi.org/10.1101/2020.12.28.424451.

30. Greaney, A.J., Loes, A.N., Crawford, K.H.D., Starr, T.N., Malone, K.D., Chu, H.Y., and Bloom, J.D. (2021). Comprehensive mapping of mutations to the SARS-CoV-2 receptor-binding domain that affect recognition by polyclonal human serum antibodies. bioRxiv. https://doi.org/10.1101/2020.12.31.425021.

31. Chen, R.T., Markowitz, L.E., Albrecht, P., Stewart, J.A., Mofenson, L.M., Preblud, S.R., and Orenstein, W.A. (1990). Measles antibody: reevaluation of protective titers. J. Infect. Dis. *162*, 1036–1042.

32. Zingher, A., and Mortimer, P. (2005). Convalescent whole blood, plasma and serum in the prophylaxis of measles: JAMA, 12 April, 1926; 1180-1187. Rev. Med. Virol. *15*, 407–418, discussion 418–421.

33. Lin, W.H., Pan, C.H., Adams, R.J., Laube, B.L., and Griffin, D.E. (2014). Vaccine-induced measles virus-specific T cells do not prevent infection or disease but facilitate subsequent clearance of viral RNA. MBio *5*, e01047.

34. de Swart, R.L., Vos, H.W., UytdeHaag, F.G., Osterhaus, A.D., and van Binnendijk, R.S. (1998). Measles virus fusion protein- and hemagglutinin-transfected cell lines are a sensitive tool for the detection of specific antibodies by a FACS-measured immunofluorescence assay. J. Virol. Methods *71*, 35–44.

35. Ziegler, D., Fournier, P., Berbers, G.A., Steuer, H., Wiesmüller, K.H., Fleckenstein, B., Schneider, F., Jung, G., King, C.C., and Muller, C.P. (1996). Protection against measles virus encephalitis by monoclonal antibodies binding to a cystine loop domain of the H protein mimicked by peptides which are not recognized by maternal antibodies. J. Gen. Virol. *77*, 2479–2489.

36. Bouche, F.B., Ertl, O.T., and Muller, C.P. (2002). Neutralizing B cell response in measles. Viral Immunol. *15*, 451–471.

37. Ertl, O.T. (2003). Immunodominant region and novel functional domains of the measles virus hemagglutinin protein (Tübingen University), PhD thesis.

38. Ertl, O.T., Wenz, D.C., Bouche, F.B., Berbers, G.A., and Muller, C.P. (2003). Immunodominant domains of the Measles virus hemagglutinin protein eliciting a neutralizing human B cell response. Arch. Virol. *148*, 2195–2206.

39. Truong, A.T., Kreis, S., Ammerlaan, W., Hartter, H.K., Adu, F., Omilabu, S.A., Oyefolu, A.O., Berbers, G.A., and Muller, C.P. (1999). Genotypic and antigenic characterization of hemagglutinin proteins of African measles virus isolates. Virus Res. *62*, 89–95.

40. Fournier, P., Brons, N.H., Berbers, G.A., Wiesmüller, K.H., Fleckenstein, B.T., Schneider, F., Jung, G., and Muller, C.P. (1997). Antibodies to a new linear site at the topographical or functional interface between the haemagglutinin and fusion proteins protect against measles encephalitis. J. Gen. Virol. *78*, 1295–1302.

41. Sheshberadaran, H., Chen, S.N., and Norrby, E. (1983). Monoclonal antibodies against five structural components of measles virus. I. Characterization of antigenic determinants on nine strains of measles virus. Virology *128*, 341–353.

42. Iankov, I.D., Penheiter, A.R., Griesmann, G.E., Carlson, S.K., Federspiel, M.J., and Galanis, E. (2013). Neutralization capacity of measles virus H protein specific IgG determines the balance between antibody-enhanced infectivity and protection in microglial cells. Virus Res. *172*, 15–23.

43. Giraudon, P., and Wild, T.F. (1985). Correlation between epitopes on hemagglutinin of measles virus and biological activities: passive protection by monoclonal antibodies is related to their hemagglutination inhibiting activity. Virology *144*, 46–58.

44. Cathomen, T., Naim, H.Y., and Cattaneo, R. (1998). Measles viruses with altered envelope protein cytoplasmic tails gain cell fusion competence. J. Virol. *72*, 1224–1234.

45. von Messling, V., Zimmer, G., Herrler, G., Haas, L., and Cattaneo, R. (2001). The hemagglutinin of canine distemper virus determines tropism and cytopathogenicity. J. Virol. *75*, 6418–6427.

46. Muñoz-Alía, M.A., and Russell, S.J. (2019). Probing Morbillivirus Antisera Neutralization Using Functional Chimerism between Measles Virus and Canine Distemper Virus Envelope Glycoproteins. Viruses *11*, 688.

47. de Swart, R.L., Yüksel, S., and Osterhaus, A.D. (2005). Relative contributions of measles virus hemagglutinin- and fusion protein-specific serum antibodies to virus neutralization. J. Virol. *79*, 11547–11551.

48. Ono, N., Tatsuo, H., Hidaka, Y., Aoki, T., Minagawa, H., and Yanagi, Y. (2001). Measles viruses on throat swabs from measles patients use signaling lymphocytic activation molecule (CDw150) but not CD46 as a cellular receptor. J. Virol. *75*, 4399–4401.

49. von Messling, V., Springfeld, C., Devaux, P., and Cattaneo, R. (2003). A ferret model of canine distemper virus virulence and immunosuppression. J. Virol. *77*, 12579–12591.

50. Nakamura, T., Peng, K.W., Vongpunsawad, S., Harvey, M., Mizuguchi, H., Hayakawa, T., Cattaneo, R., and Russell, S.J. (2004). Antibody-targeted cell fusion. Nat. Biotechnol. *22*, 331–336.

51. Tatsuo, H., Ono, N., Tanaka, K., and Yanagi, Y. (2000). SLAM (CDw150) is a cellular receptor for measles virus. Nature *406*, 893–897.

52. Peng, K.W., Ahmann, G.J., Pham, L., Greipp, P.R., Cattaneo, R., and Russell, S.J. (2001). Systemic therapy of myeloma xenografts by an attenuated measles virus. Blood *98*, 2002–2007.

53. Mrkic, B., Pavlovic, J., Rülicke, T., Volpe, P., Buchholz, C.J., Hourcade, D., Atkinson, J.P., Aguzzi, A., and Cattaneo, R. (1998). Measles virus spread and pathogenesis in genetically modified mice. J. Virol. *72*, 7420–7427.

54. del Valle, J.R., Devaux, P., Hodge, G., Wegner, N.J., McChesney, M.B., and Cattaneo, R. (2007). A vectored measles virus induces hepatitis B surface antigen antibodies while protecting macaques against measles virus challenge. J. Virol. *81*, 10597–10605.

55. Ishikawa, H., Meng, F., Kondo, N., Iwamoto, A., and Matsuda, Z. (2012). Generation of a dual-functional split-reporter protein for monitoring membrane fusion using self-associating split GFP. Protein Eng. Des. Sel. *25*, 813–820.

56. Bohm, M., Bohne-Lang, A., Frank, M., Loss, A., Rojas-Macias, M.A., and Lutteke, T. (2019). Glycosciences.DB: an annotated data collection linking glycomics and proteomics data (2018 update). Nucleic Acids Res. *47*, D1195–D1201.

57. Gonçalves-Carneiro, D., McKeating, J.A., and Bailey, D. (2017). The Measles Virus Receptor SLAMF1 Can Mediate Particle Endocytosis. J. Virol. *91*, e02255, 16.

58. Zhang, X., Wallace, O.L., Domi, A., Wright, K.J., Driscoll, J., Anzala, O., Sanders, E.J., Kamali, A., Karita, E., Allen, S., et al. (2015). Canine distemper virus neutralization activity is low in human serum and it is sensitive to an amino acid substitution in the hemagglutinin protein. Virology *482*, 218–224.

59. Parks, C.L., Lerch, R.A., Walpita, P., Sidhu, M.S., and Udem, S.A. (1999). Enhanced measles virus cDNA rescue and gene expression after heat shock. J. Virol. *73*, 3560–3566.

60. Radecke, F., Spielhofer, P., Schneider, H., Kaelin, K., Huber, M., Dötsch, C., Christiansen, G., and Billeter, M.A. (1995). Rescue of measles viruses from cloned DNA. EMBO J. *14*, 5773–5784.

61. Beaty, S.M., Park, A., Won, S.T., Hong, P., Lyons, M., Vigant, F., Freiberg, A.N., tenOever, B.R., Duprex, W.P., and Lee, B. (2017). Efficient and Robust *Paramyxoviridae* Reverse Genetics Systems. MSphere *2*, e00376, 16.

62. Saw, W.T., Matsuda, Z., Eisenberg, R.J., Cohen, G.H., and Atanasiu, D. (2015). Using a split luciferase assay (SLA) to measure the kinetics of cell-cell fusion mediated by herpes simplex virus glycoproteins. Methods *90*, 68–75.

63. Haralambieva, I.H., Ovsyannikova, I.G., O'Byrne, M., Pankratz, V.S., Jacobson, R.M., and Poland, G.A. (2011). A large observational study to concurrently assess persistence of measles specific B-cell and T-cell immunity in individuals following two doses of MMR vaccine. Vaccine *29*, 4485–4491.

64. Hu, A., Sheshberadaran, H., Norrby, E., and Kövamees, J. (1993). Molecular characterization of epitopes on the measles virus hemagglutinin protein. Virology *192*, 351–354.

65. Massé, N., Ainouze, M., Néel, B., Wild, T.F., Buckland, R., and Langedijk, J.P. (2004). Measles virus (MV) hemagglutinin: evidence that attachment sites for MV receptors SLAM and CD46 overlap on the globular head. J. Virol. *78*, 9051–9063.

66. Liu, F., Song, Y., and Liu, D. (1999). Hydrodynamics-based transfection in animals by systemic administration of plasmid DNA. Gene Ther. *6*, 1258–1266.

STAR★METHODS

KEY RESOURCES TABLE

REAGENT or RESOURCE	SOURCE	IDENTIFIER
Antibodies		
F3-5	Rik L. de Swart	[34]
C28-10	Rik L. de Swart	[34]
BH006	Claude P. Muller	[35]
BH130	Claude P. Muller	[36]
BH097	Claude P. Muller	[36]
BH094	Claude P. Muller	[37]
BH015	Claude P. Muller	[38]
BH089	Claude P. Muller	[38]
BH021	Claude P. Muller	[35]
BH125	Claude P. Muller	[39]
BH030	Claude P. Muller	[38]
BH216	Claude P. Muller	[35]
BH101	Claude P. Muller	[38]
BH129	Claude P. Muller	[40]
BH059	Claude P. Muller	[40]
BH068	Claude P. Muller	[37]
BH047	Claude P. Muller	[37]
BH026	Claude P. Muller	[36]
BH031	Claude P. Muller	[36]
BH067	Claude P. Muller	[36]
BH081	Claude P. Muller	[36]
BH038	Claude P. Muller	[36]
BH141	Claude P. Muller	[36]
BH017	Claude P. Muller	[37]
Anti-measles blend, clones CV1, CV4	Millipore-Sigma	Cat# MAB8905, RRID:AB_95486
16DE6	M. Ehnlund	[41]
I44	M. Ehnlund	[41]
I41	M. Ehnlund	[41]
I29	M. Ehnlund	[41]
20H6	Ianko Iankov	[42]
Cl55	Patricia Devaux	[43]
Cl48	Mark J. Federspiel	[43]
Anti-MeV-N, clone 83KKII	Millipore-Sigma	Cat# MAB8906, RRID:AB_2147180
Human SLAM/150 PE-conjugated	R&D Systems	Cat# FAB1642P, RRID:AB_1655770
Human CD46 PE-conjugated	R&D Systems	FAB2005P, RRID:AB_2074803
Human nectin-4 PE-conjugated	R&D Systems	FAB2659P, RRID:AB_2174291
Mouse IgG2b PE-conjugated	R&D Systems	Cat# IC0041P, RRID:AB_357249
Mouse anti-FLAG M2	Millipore-SIGMA	Cat# F3165, RRID:AB_259529
Anti-β actin, peroxidase-conjugated	Millipore-SIGMA	Cat# A3854, RRID:AB_262011
Rabbit anti-MeV-H cytoplasmic tail	Kah Whye Peng	[44]
Rabbit anti-F cytoplasmic tail	Veronika Von Messling	[45]
Goat anti-rabbit IgG, peroxidase-conjugated	ThermoFisher	Cat# 31462, RRID:AB_228338
Goat anti-mouse IgG, peroxidase-conjugated	ThermoFisher	Cat# 62-6520, RRID:AB_2533947

(*Continued on next page*)

Continued

REAGENT or RESOURCE	SOURCE	IDENTIFIER
Bacterial and virus strains		
Escherichia coli MAX Efficiency stbl2	ThermoFisher	10268019
MeVvac2(GFP)N	Stephen J. Russell's laboratory stock	[46]
MeVvac2(GFP)N CDV H/F	This paper	N/A
MeVvac2(GFP)N MeV-H/CDV-F	This paper	N/A
MeVvac2(GFP)N CDV-H/MeV-F	This paper	N/A
MeVvac2(GFP)N MeV-H genotype B3.1	Stephen J. Russell's laboratory stock	[16]
MeVvac2(GFP)N MeV-H genotype D4.1	Stephen J. Russell's laboratory stock	[18]
MeVvac2(GFP)N MeV-H genotype D8	Stephen J. Russell's laboratory stock	[16]
MeVvac2(GFP)N MeV-H genotype D9	Stephen J. Russell's laboratory stock	[16]
MeVvac2(GFP)N MeV-H genotype G3	Stephen J. Russell's laboratory stock	[16]
MeVvac2(GFP)N MeV-H genotype H1 (MeV-H1)	Stephen J. Russell's laboratory stock	[16]
MeVvac2(GFP)N MeV-H1 N481Y	This paper	N/A
MeVvac2(GFP)N MeV-H1 H495R	This paper	N/A
MeVvac2(GFP)N MeV-H1 H495R/S546G	This paper	N/A
MeVvac2(GFP)N MeV-H1 N481Y/H495R	This paper	N/A
MeVvac2(GFP)N MeV-H1 N481Y/S546G	This paper	N/A
MeVvac2(GFP)N MeV-H1 N481Y/H495R/S546G	This paper	N/A
MeVvac2(GFP)P	This paper	N/A
MeVvac2(Fluc)P	This paper	N/A
MeVvac2(GFP)P MeV-H1	This paper	N/A
MeVvac2(GFP)P MeV-HΔ8 (see table S1)	This paper	N/A
MeVvac2(GFP)P MeV-HΔ7 Ia	This paper	N/A
MeVvac2(GFP)P MeV-HΔ7 Ib	This paper	N/A
MeVvac2(GFP)P MeV-HΔ7 IIa	This paper	N/A
MeVvac2(GFP)P MeV-HΔ7 IIb	This paper	N/A
MeVvac2(GFP)P MeV-HΔ7 IIc	This paper	N/A
MeVvac2(GFP)P MeV-HΔ7 III	This paper	N/A
MeVvac2(GFP)P MeV-HΔ7 Ø	This paper	N/A
MeVvac2(GFP)P MeV-HΔ8/ CDV-F	This paper	N/A
MeVvac2(Fluc)P MeV-HΔ8/ CDV-F	This paper	N/A
Biological samples		
Guinea pig anti-measles virus	BEI Reources	NR-4024
Ferret anti-canine distemper virus	BEI Reources	NR-4025
Mouse anti-MeV-H (genotype A)	This paper	NR-4025
Rabbit anti-MeV-H (genotype A)	Stephen J. Russell's laboratory stock	[17]
Anti-measles serum (3rd international standard)	NIBSC	97/648
Human AB serum	Valley Biomedical Products and Services, Inc	HS1017, (Lot #C80553)
Human sera from Dutch individuals	Rik L. de Swart's laboratory stock	[47]
Human sera from Olmstead county individuals	Mayo Clinic Biobank	N/A
Human sera from Hispanic individuals	Innovative Research Inc	N/A
Chemicals, peptides, and recombinant proteins		
DMEM	GE Healthcare Life Science	SH30022.01
RPMI 1640 medium	Corning Inc	10-040-CV
DMEM-F12	ThermoFisher	11330-021

(*Continued on next page*)

Continued

REAGENT or RESOURCE	SOURCE	IDENTIFIER
Opti-MEM I reduced serum media	ThermoFisher	31985070
Penicillin/Streptomycin	Corning Inc	30-002-CI
Fetal bovine serum	ThermoFisher	10437-028
HEPES	Life Technologies	15630-080
Geneticin	Mediatech Inc	MT-61-234-RG
Zeocin	InvivoGen	ant-zn-1
1 × Halt protease and phosphatase inhibitor cocktail	Thermo Fisher	78441
Radioimmunoprecipitation assay buffer	Abcam	ab156034
Restriction enzymes	New England Biolabs	N/A
Fugene HD	PROMEGA	E2311
EnduRen live cell substrate	PROMEGA	E6481
Versene	ThermoFisher	15040066
Recombinant SLAMF1-Fc	Stephen J. Russell's laboratory stock	[16]
Recombinant Nectin-4-Fc	Stephen J. Russell's laboratory stock	[16]
Recombinant CD46-Fc	This paper	N/A
Recombinant MeV-H (genotype A)	Stephen J. Russell's laboratory stock	[16]
Recombinant MeV-HΔ8	This paper	N/A
Recombinant nucleocapsid	CD Creative Diagnostics	DAG-P2862
DTSSP (sulfosuccinimidyl propionate)	ThermoFisher	21578
EZview red protein G affinity gel	Millipore-SIGMA	E3403
1-step Ultra TMB	ThermoFisher	34028
D-Luciferin	GoldBio	LUCK-100
Critical commercial assays		
QuickChange-site directed mutagenesis kit	Agilent	200514
BD Quantibrite Beads	BD Biosciences	340495
Expi293 expression system	ThermoFisher	A14635
Experimental models: cell lines		
African green monkey: Vero	ATCC	CCL-81
African green monkey: Vero/human SLAMF1	Yusuke Yanagi	[48]
African green monkey: Vero/dog SLAM tag	Roberto Cattaneo	[49]
Hamster: BHK	ATCC	CCL-10
Hamster: CHO	C. Richardson	N/A
Hamster: CHO-CD46	Stephen J. Russell's laboratory stock	[50]
Hamster: CHO-nectin4	Kah-Whye Peng	[20]
Hamster: CHO-SLAMF1	Yusuke Yanagi	[51]
Human: Mel-JuSo/wt	Rik L. de Swart	[34]
Human: Mel-JuSo-/MeV-H	Rik L. de Swart	[34]
Human: Mel-JuSo-/MeV-F	Rik L. de Swart	[34]
Human: HEK293	François-Loïc Cosset	N/A
Human: KAS 6/1	R. Fonseca and D.F. Jelinek	[52]
Human: Expi293F	ThermoFisher	A14527
Experimental models: organisms/strains		
Mouse: Ifnar^{tm}-CD46Ge	Mayo Clinic Breeding colony	[53]
Mouse: C.B-17 scid	Taconic	Cat# TAC:cb17sc, RRID:IMSR_TAC:cb17sc
Mouse: C57BL/6J	The Jackson Laboratory	Cat# JAX:000664, RRID:IMSR_JAX:000664

(*Continued on next page*)

Continued

REAGENT or RESOURCE	SOURCE	IDENTIFIER
Recombinant DNA		
pSMART-MeVvac2(GFP)N	Stephen J. Russell's laboratory stock	[46]
pB(+)MeVvac2(ATU)P	Roberto Cattaneo	[54]
pSMART-MeVvac2(GFP)P	This paper	N/A
MeVvac2(GFP)N MeV-H1 N481Y	This paper	N/A
MeVvac2(GFP)N MeV-H1 H495R	This paper	N/A
MeVvac2(GFP)N MeV-H1 H495R/S546G	This paper	N/A
MeVvac2(GFP)N MeV-H1 N481Y/H495R	This paper	N/A
MeVvac2(GFP)N MeV-H1 N481Y/S546G	This paper	N/A
MeVvac2(GFP)N MeV-H1 N481Y/495R/S546G	This paper	N/A
MeVvac2(GFP)P encoding MeV-HΔ8	This paper	N/A
MeVvac2(GFP)P encoding MeV-HΔ7 Ia	This paper	N/A
MeVvac2(GFP)P encoding MeV-HΔ7 Ib	This paper	N/A
MeVvac2(GFP)P encoding MeV-HΔ7 IIa	This paper	N/A
MeVvac2(GFP)P encoding MeV-HΔ7 IIb	This paper	N/A
MeVvac2(GFP)P encoding MeV-HΔ7 IIc	This paper	N/A
MeVvac2(GFP)P encoding MeV-HΔ7 III	This paper	N/A
MeVvac2(GFP)P encoding MeV-HΔ7 Ø	This paper	N/A
MeVvac2(GFP)P encoding MeV-HΔ8/CDV-F	This paper	N/A
MeVvac2(Fluc)P encoding MeV-HΔ8/CDV-F	This paper	N/A
MeVvac2(GFP)N encoding CDV H/F	This paper	N/A
MeVvac2(GFP)N encoding MeV-H/CDV-F	This paper	N/A
MeVvac2(GFP)N encoding CDV-H/MeV-F	This paper	N/A
pCG-Hol	Roberto Cattaneo	[45]
pCG-Hol Y537D	This paper	N/A
pCG-Fol	Roberto Cattaneo	[45]
pCG-Fol L466F	This paper	N/A
pCG-H	Roberto Cattaneo	[44]
pCG-F	Roberto Cattaneo	[44]
pCG-H MeV-H1	Stephen J. Russell's laboratory stock	[16]
pCG-H MeV-H1 N481Y	This paper	N/A
pCG-H MeV-H1 H495R	This paper	N/A
pCG-H MeV-H1 H495R/S546G	This paper	N/A
pCG-H MeV-H1 N481Y/S546G	This paper	N/A
pCG-H (MeV-H1 N481Y/H495R/S546G	This paper	N/A
pCG-H MeV-H1 Δ8 (see table S1)	This paper	N/A
pCG-H MeV-H1) Δ8 A165T	This paper	N/A
pCG-H MeV-H1 Δ8 E379G	This paper	N/A
pCG-H MeV-H1 Δ8 A165T/E379G	This paper	N/A
pCG-H MeV-H1 Δ7 Ia	This paper	N/A
pCG-H MeV-H1 Δ7 Ib	This paper	N/A
pCG-H MeV-H1 Δ7 IIa	This paper	N/A
pCG-H MeV-H1 Δ7 IIb	This paper	N/A
pCG-H MeV-H1 Δ7 IIc	This paper	N/A
pCG-H MeV-H1 Δ7 III	This paper	N/A
pCG-H MeV-H1 Δ7 Ø	This paper	N/A
Rluc8155-15DSP1-7	Zene Matsuda	[55]

(*Continued on next page*)

Continued

REAGENT or RESOURCE	SOURCE	IDENTIFIER
Rluc8 155-156 DSP 8-11	Zene Matsuda	[55]
pFUSE-hIgG1e3-Fc1-CD46	This paper	N/A
Software and algorithms		
The PyMOL Molecular Graphics System, Version 2.0	Schrödinger, LLC	https://pymol.org/2/
Glycoscienes.DB	[56]	http://www.glycosciences.de
GraphPad Prism version 8.4.2 for macOS	GraphPad	https://www.graphpad.com:443/

RESOURCE AVAILABILITY

Lead contact

Further information and request for resources and reagents should be directed to and will be fulfilled by the Lead Contact, Stephen J. Russell, MD, PhD (sjr@mayo.edu)

Materials availability

All unique reagents generated in this study are available from the Lead Contact with a completed Materials Transfer Agreement.

Data and code availability

The datasets supporting the current study are available from the corresponding author on request.

EXPERIMENTAL MODEL AND SUBJECT DETAILS

Biosafety Statement

Although the modified envelope glycoprotein complex generated in this project could be theoretically implanted into a pathogenic measles virus, doing so would destroy its ability to interact with SLAMF1 and nectin-4, the two receptors used by pathogenic measles viruses (and by all other pathogenic morbilliviruses) to cause disease. To restore these pathogenicity-determining tropisms, a major antigenic site would be reintroduced into the H glycoprotein of the hypothetical virus, thereby rendering it fully susceptible to measles-immune human serum.

Human samples

Human serum samples were from 3 cohorts. Cohort 1 samples were obtained from the Erasmus Medical Center serum bank and have been previously described.[47] Members of cohort 1 likely were never exposed to wild-type MeV and likely received a monovalent measles vaccination at age 14 months and a measles-mumps-rubella (MMR) vaccination at age 9 years. Cohort 2 samples were obtained from the Mayo Clinic Biobank in Olmsted County (Rochester, MN) following institutional review board (IRB) approval; this region has no documented evidence of circulating measles or rubella virus in the past and has high vaccine coverage. However, MMR vaccination status was not available for most samples. The subjects' age for cohort 2 ranged from 30 to 44 years, and 80% were female. Serum samples were tested by enzyme-linked immunosorbent assay for IgG antibodies specific to MeV and rubella virus, and no differences were identified between those with 1 documented dose of MMR and those without vaccination documented. Cohort 3 samples were custom purchased from Innovative Research Inc, based on age and race. Hispanic donors between 20 and 29 years old were chosen to increase the likehood of obtaining serum samples from vaccinated people. The Latin America region was the first in the world to have eliminated measles and people in that age range were considered to have acquired their MeV protection exclusively through vaccination without further boosting of immunity through exposure to wild-type viruses. All serum samples were heat inactivated.

Cells and viruses

Vero cells (CCL-81, ATCC, Masassas, VA, USA) and Vero cells stably transfected with human SLAMF1[48] or with its canine counterpart[49] were grown in Dulbecco's modified minimal essential medium (DMEM) (HyClone, GE Healthcare Life Science, Marlborough, MA, USA) supplemented with 5% (vol./vol.) heat-inactivated fetal bovine serum (ThermoFisher Scientific, Whaltham, MA, USA) and 0.5 mg/mL of geneticin (G418; Corning Inc., Manassas, VA) for Vero/hSLAMF1 or 1 mg/mL zeocin (ThermoFisher Scientific) for Vero/cSLAMF1. CHO cells, CHO-CD46,[50] CHO-SLAMF1[51] and CHO-nectin4[20] were cultured as previously described. Baby hamster kidney cells were maintained in DMEM-10% fetal bovine serum. The human melanoma Mel-JuSo cell line and derivatives, transfected with the full-length MeV-F and MeV-H genes (Mel-JuSo-F or Mel-JuSo-H) were cultured in RPMI 1640 medium (Corning Inc.) supplemented with G418.

Viruses have been named according to the genotype of MeV-H gene expressed and were propagated as described previously.[16,19] For mouse inoculation, viruses were purified through a sucrose gradient as described elsewhere.[57]

Organism

The transgenic mice (Ifnar^{tm}-CD46Ge) expressing the human CD46 were obtained from Dr. Roberto Cattaneo's lab.[53] Ifnar^{tm}-CD46Ge were bred and maintained in specific pathogen free (SPF) environment at the Department of Comparative Medicine, Institute Hills Research Facility of Mayo Clinic. Males and females at four to eight weeks-old were used in this study. Female C.B-17 SCID mice of 4-6 weeks old were purchased from Taconic (Germantown, NY, USA). Viral infections were performed in an animal biosafety level 2+ in adherence with the guidelines from the Department of Comparative Medicine and the Institutional Biosafety Committee. Female C57BL/6J mice of 4-6 weeks old were purchased form The Jackson Laboratory (Bar Harbor, ME, USA)

METHOD DETAILS

Prior to the onset of experimentation, the Mayo Clinic Institutional Biosafety Committee (IBC) performed a Dual Use Research of Concern (DURC) evaluation on the proposed project. Although it flagged as a project with DURC elements, the project was allowed to continue with work occurring in a certified Biosafety Level 2/2+ facility and with ongoing oversight by the Biosafety Office. Despite tremendous mutational pressure, evidence that there are mutations in the viral H and N genes, and widespread infections throughout geography and time, the virus has remained monotypic. Given those elements, it was the view of the authors and the institutional review team that there was an unknown factor protecting the monotypic status of the vaccine strain which decreased the concern that the work proposed by this project would result in a virus that could pose increased public risk. Had evidence arising during the course of the project that would have altered that determination, an additional review of the project would have been conducted.

Constructs and rescue of recombinant MeVs

Viruses used in this study were derived from the molecular cDNA clone of the Moraten/Schwartz vaccine strain. For the construction of recombinant MeVs, pSMART LC MeV^{vac2}(eGFP)N plasmid,[46] encoding for a rMeV expressing the enhanced green fluorescent protein (eGFP) upstream of the N gene, and pB(+)MeV^{vac2}(ATU)P, plasmid encoding for a rMeV with an additional transcription unit (ATU) downstream of the phosphoprotein gene,[54] were used. A DNA fragment encoding for firefly luciferase (Fluc, GenBank accession #KF926476) with Mlu/AatII restriction sites at its extremities, was then cloned into the corresponding sites of the ATU to obtain pB(+)MeV^{vac2}(Fluc)P. To avoid plasmid instability during propagation in bacteria, *Escherichia coli* Stbl2 cells (ThermoFisher Scientific) were used (grown at 30°C).

We used the CDV Ondersterpoort vaccine strain H (CDV-H) and F (CDV-F) genes, originally contained in pCG plasmid,[45] to produce envelope-exchange MeVs. To replace MeV-H from the MeV backbone, site-directed mutagenesis (QuikChange site-directed mutagenesis kit, Agilent, Santa Clara, CA, USA) was used to remove a SpeI site in CDV-H, and a Y537D substitution was then introduced, which reduces binding by crossreactive nAb in human sera.[58] PacI and SpeI restriction sites (underlined) were introduced into the beginning and end of the gene, respectively, by polymerase chain reaction using forward primer 5′-ttaattaaacttagggtgcaagatca tcgataatgctcccctaccaagacaagg-3′ and reverse primer 5′-actagtgggtatgcctgatgtctgggtgacatcatgtgattggttcactagcagccttaatggtgg tgatggtggtggctccccctgcggccgcggccggctgggccgctctaccctcgatacggttacatgagaatcttatacggac-3′, leaving the untranslated region unchanged. The PCR product was digested with PacI and SpeI and cloned into the MeV backbone. To replace MeV-F from the MeV antigenome plasmid, pCG-CDV-F was digested with HpaI/SpeI and inserted into similarly digested pCG-MeV-F. The NarI/SpeI fragment of this plasmid was then used to replace that of MeV.

The recovery of recombinant MeVs was performed as previously described.[59–61]

Fusion assay

Cells (5×10^5 cells/well in a 6-well plate) were cotransfected using Fugene HD (Promega, Madison, WI, USA) with 1 μg of pCG plasmid encoding vaccine strain MeV-F and pCG encoding the appropriate MeV-H. Fusion activity was evaluated 24 hours later.

To quantify cell fusion, we used the dual-split luciferase assay as previously described.[62] Briefly, effector baby hamster kidney cells ($3 \times 10^{4\ cells}$) in black 96-well plates were cotransfected with 33 ng each of the MeV-H and MeV-F expression plasmids and one of the split luciferase plasmids, DSP_{8-11}. As a control, only the MeV-F and DSP_{8-11} plasmids were transfected. CHO cells and CHO cells expressing the respective MeV receptors (2×10^5 cells/well in 6-well plates) were transfected with 1.5 μg of the other dual-split-reporter plasmid (DSP_{1-7}). Twenty-four hours after transfection, target cells were detached with Versene (ThermoFisher Scientific) and cocultured with the effector cells in Fusion media (DMEM-F12 without Phenol Red + 40 mM HEPES), supplemented with 1:1000 dilution of the cell-permeable luciferase substrate EnduREN (Promega). Luminescence resulting from cell fusion and mixing of cytoplasmic content between target and effector cells was monitored with a Topcount NXT Luminometer (Packard Instrument Company, Meriden, CT) at the indicated time points. The data shown are the mean and standard deviation of 3 replicates for each H plasmid.

Fluorescence-activated cell sorting analysis and quantification of cell surface molecules

Cells were washed and detached by using Versene and immediately incubated with phycoerythrin-conjugated antibodies: anti-SLAMF1 (R&D Systems, Minneapolis, MN, USA), anti-CD46 (R&D Systems), anti-nectin4 (R&D Systems), or control isotype antibody

(R&D Systems). After a 1-hour incubation at 4°C, cells were washed again and fluorescence was measured in a FACSCanto flow cytometry system (BD Bioscience, Franklin Lakes, NJ, USA). The number of receptors per cell was estimated with calibration beads (BD QuantiBRITE; BD Biosciences) as the reference standard.

Recombinant proteins and binding assays

The coding sequence of the CD46 ectodomain (residues 35-328) was amplified via PCR from pGEM-CD46 vector (Sino Biologicals Inc., Beijing, China.) and inserted into a pFUSE vector (pfc1-hg1e3; Invivogen San Diego, CA, USA) in frame with the murine Ig κ-chain leader sequence and a 3C protease cleavage sequence at the 5′ end of the Fc region using In-Fusion cloning kit (Clontech, Mountain View, CA, USA). CD46-Fc, SLAM-Fc,[16] and nectin4-Fc[16] recombinant proteins were expressed in Expi293F cells (ThermoFisher Scientific) and purified from culture supernatant as previously described.[16]

The expression and purification of recombinant soluble MeV-H were performed as previously described.[18]

Binding of the receptors-Fc to MeV-H was determined by enzyme-linked immunosorbent assay as previously described.[16] The absorbance at 450 nm was measured with an Infinite M200Pro microplate reader (Tecan). The data were analyzed using Prism software (GraphPad) and adjusted to a 1-site binding saturation mode, which showed excellent fit ($R^2 > 0.99$).

Assessment of F interaction with H proteins

Three micrograms (1 μg of H and 2 μg of F) of total DNA were transfected into HEK293T cells ($4x10^5$ cells). After 24 h, the cells were washed twice with PBS and treated with the cross-linker 3-3′-diothiobis (sulfosuccinimidyl propionate) (Thermo Fisher Scientific) at 1 mM, followed by quenching with 20 mM Tris/HCl (pH 7.4) and lysis with 0.4 mL of 1X radio-immunoprecipitation (RIPA) buffer (Abcam, Cambridge, MA, USA) containing a 1 × Halt protease and phosphatase inhibitor cocktail (ThermoFisher Scientific). Soluble fractions were collected after centrifugation at 10,000 x g for 10 min at 4°C, and one-thirtieth of the volume was set aside as the cell lysate input. The rest was incubated with 0.5 μg of anti-FLAG monoclonal antibody M2 (Sigma-Aldrich, St. Louis, MO, USA) and EZview red protein G affinity gel (Sigma-Aldrich). The precipitated material was washed (20 mM Tris-HCl, pH 7.4, 140 mM sodium chloride) and denatured by heating in laemmli buffer containing β-mercaptoethanol, fractionated into 4%–12% Bis-Tris polyacrylamide gel, and transferred to polyvinylidene fluoride membranes. Blots were analyzed with anti-MeV-Hcyt,[44] anti-F,[45] and mouse anti–β -actin[16,46] and probed with a conjugated secondary rabbit antibody (ThermoFisher Scientific). The blots were incubated with SuperSignal West Pico chemiluminescent substrate (ThermoFisher Scientific) and analyzed with a ChemiDoc Imaging Sytem (Bio-Rad, Hercules, CA, USA).

Passive Immunization and *In Vivo* Imaging

Neutralizing antibodies (600 mIU) were administered in the form of anti-serum and they were obtained through the NIH Biodefense and Emerging Infections Research Resources Repository, NIAID, NIH: Polyclonal Anti-Measles Virus, Edmonston, (antiserum, Guinea pig), NR-4024; and polyclonal anti–CDV, Lederle avirulent (antiserum, ferret), NR-4025. We have previously determined their specificity and potency of the reagents.[46] Ifnar^{tm}-CD46Ge mice[53] received intra-peritoneally virus anti-serum 3 hours before injection of $2x10^5$ $TCID_{50}$/100 μL of rMeV(Fluc)P viruses, following the same route. At 24, 48, 72 and 96 hours, mice were anesthetized and inoculated with D-Luciferin (GoldBio, St Louis, MO, USA) 15 min before *in vivo* imaging of bioluminescence using an IVIS Spectrum instrument (PerkinElmer, Waltham, MA, USA). Female CB17 ICR SCID mice of 4-6 weeks old were purchased from Taconic (Germantown, NY, USA) and implanted subcutaneously with $1x10^7$ KAS 6/1 cells one day after whole body irradiation (2Gy). When tumor reached a volume of 0.5 cm^3, $2x10^5$ $TCID_{50}$ units of rMeV(Fluc)P viruses or 100 μL of PBS were injected through the tail vein. *In vivo* imaging was then recorded as described previously.

Serologic Assays

Virus neutralization assays were based on the fluorescence-based PRMN assay, as previously described.[16,18,19] Alternatively, a luciferase-based neutralization assays was developed. After incubation for 72 h at 37°C and 5% CO_2, 100 μL of DMEM/F-12 (ThermoFisher Scientific) containing 0.5 mM of D-Luciferin was added to each well of a black 96-well plate. Luciferase-expressing cells were quantified with an Infinite M200 Pro multimode microplate reader (Tecan Trading AG). Each assay was repeated at least twice and on different days, with 4 replicates per assay. Antibody concentration required to inhibit viral infection by 50% (neutralizing antibody titer at 50% inhibition) was calculated after fitting the data to a sigmoidal dose-response (variable slope) with GraphPad software (Prism 7). Values were converted to mIU/mL by using the third World Health Organization international anti-measles standard, as previously described.[63]

Rabbit anti-MeV-H sera were generated by immunization with adenovirus expressing the MeV-H from the vaccine strain.[17]

Murine monoclonal anti-MeV-H antibodies were produced and characterized as previously described.[19,35,37,40,64,65] Polyclonal antibodies were generated by gene-based hydrodynamic injection[66] of C57BL/6 mice with 20 μg of plasmid DNA or by intraperitoneal inoculation of mice with 1 dose of 10^5 fluorescence forming units (FFU) of MeV-expressing GFP. Serum was obtained 4 weeks after inoculation.

Estimation of MeV-N antibodies were performed by enzyme-linked immunosorbent assay using a nucleocapsid protein as the antigen. A standard calibration curve was generated with anti-MeV-N (clone 83KKII; MilliporeSigma, Burlington, MA, USA).

Structural Modeling

A model of the MeV-H was generated from the crystallographic structures of the MeV-H alone (PDB 2ZB5) and the MeV-H-SLAMF1 complex (PDB 3ALZ). The model was then submitted for *in silico* glycosylation using the GlyPro server (http://www.glycosciences.de), which produced a complex penta-antennary N-glycan model at all predicted N-glycosylation sites, including N168 and N187, that are part of disordered regions. The structures were superimposed and manipulated with PyMOL software (https://pymol.org/2/).

QUANTIFICATION AND STATISTICAL ANALYSIS

Statistical significance was calculated with GraphPad Prism 7 following the appropriate statistical test, as described in the text corresponding to each figure.